
IMPLICIT REGULARIZATION OF MULTI-TASK LEARNING AND FINETUNING IN OVERPARAMETERIZED NEURAL NETWORKS

A PREPRINT

✉ **Jack W. Lindsey**^{1,2,3} and ✉ **Samuel Lipp**^{1,2,4}

¹Center for Theoretical Neuroscience, Zuckerman Mind Brain Behavior Institute, Columbia University

²Equal contribution, random order

³jackwlindsey@gmail.com

⁴samuel.lippl@columbia.edu

March 8, 2024

ABSTRACT

In this work, we investigate the inductive biases that result from learning multiple tasks, either simultaneously (multi-task learning, MTL) or sequentially (pretraining and subsequent finetuning, PT+FT). In the simplified setting of two-layer diagonal linear networks trained with gradient descent, we apply prior theoretical results to describe novel implicit regularization penalties associated with MTL and PT+FT, both of which incentivize feature sharing between tasks and sparsity in learned task-specific features. Notably, these results imply that during finetuning, networks operate in a hybrid of the kernel (or “lazy”) regime and the feature learning (“rich”) regime identified in prior work. Moreover, we show that PT+FT can exhibit a novel “nested feature selection” behavior not captured by either regime, which biases it to extract a sparse subset of the features learned during pretraining. In ReLU networks, we reproduce all of these qualitative behaviors empirically, in particular verifying that analogues of the sparsity biases predicted by the linear theory hold in the nonlinear case. Our findings hold qualitatively for a deep architecture trained on image classification tasks, and our characterization of the nested feature selection regime motivates a modification to PT+FT that we find empirically improves performance. We also observe that PT+FT (but not MTL) is biased to learn features that are correlated with (but distinct from) those needed for the auxiliary task, while MTL is biased toward using identical features for both tasks, which can lead to a tradeoff in performance as a function of the number of finetuning samples. Our results shed light on the impact of auxiliary task learning and suggest ways to leverage it more effectively.

1 Introduction

Neural networks are often trained on multiple tasks, either simultaneously (“multi-task learning,” henceforth MTL, see [Vafaieikia et al. 2020](#); [Zhang & Yang 2022](#)) or sequentially (“pretraining” and subsequent “finetuning,” henceforth PT+FT, see [Du et al. 2022](#); [Zhou et al. 2023](#)). Empirically, models can transfer knowledge from auxiliary tasks to improve performance on tasks of interest. Understanding of how auxiliary tasks influence learning remains limited.

Auxiliary tasks are especially useful when there is less data available for the target task. Modern “foundation models,” trained on data-rich general-purpose auxiliary tasks (like next-word prediction or image generation) before adaptation to downstream tasks, are a timely example of this use case ([Bommasani et al., 2022](#)). Auxiliary tasks are also commonly used in reinforcement learning, where performance feedback can be scarce ([Jaderberg et al., 2016](#)). Intuitively, auxiliary task learning biases the target task solution to use representations shaped by the auxiliary task. When the tasks share common structure, this influence may enable generalization from relatively few training samples for the task of interest. However, it can also have downsides, causing a model to inherit undesirable biases from auxiliary task learning ([Wang & Russakovsky, 2023](#); [Steed et al., 2022](#)).

A relevant insight from the literature on single-task learning is that a combination of initialization and learning dynamics produces an implicit regularizing effect on learned solutions. This regularization can enable good generalization even when models are overparameterized (Neyshabur, 2017).

Contributions. In this work we characterize the inductive biases of MTL and PT+FT in terms of implicit regularization. Note that we focus on MTL in which feature extraction layers are shared and readouts are task-specific, and on PT+FT in which the readout of the network is reinitialized before finetuning. We first apply prior theoretical results that study a simplified “diagonal linear network” model (which importantly still captures a notion of feature learning/selection) to the settings of PT+FT and MTL. These results provide an exact description of the solutions learned by PT+FT in diagonal linear networks, and an approximate description of those learned via MTL, in terms of norm minimization biases. Both biases encourage (1) the reuse of auxiliary task features and (2) sparsity in learned task-specific features. For PT+FT, this bias corresponds to a hybrid of “rich” and “lazy” learning dynamics in different parts of the network. Additionally, we find that under suitable parameter scalings, PT+FT exhibits a novel “nested feature-selection” regime, distinct from previously characterized rich and lazy regimes, which biases finetuning to extract sparse subsets of the features learned during pretraining. In ReLU networks, we reproduce these phenomena empirically. Based on the nested feature selection insight, we suggest practical tricks to improve finetuning performance, which shows positive results in experiments. We also describe a qualitative behavior of PT+FT not captured by the linear theory: a bias toward learning main task features correlated with (but not necessarily identical to) those learned during pretraining, which we find is beneficial given sufficient training data for the task of interest but can be detrimental when data is scarce.

2 Related work

A variety of studies have characterized implicit regularization effects in deep learning. These include biases toward low-frequency functions (Rahaman et al., 2018), toward stable minima in the loss landscape (Mulayoff et al., 2021), toward low-rank solutions (Huh et al., 2023), and toward lower-order moments of the data distribution (Refinetti et al., 2023). In shallow (single hidden-layer) networks, Chizat & Bach (2020) show that when using cross-entropy loss, shallow networks are biased to minimize the \mathcal{F}_1 norm, an infinite-dimensional analogue of the ℓ_1 norm over the space of possible hidden-layer features (see also Lyu & Li, 2020; Savarese et al., 2019). Other work has shown that implicit regularization for mean squared error loss in nonlinear networks cannot be exactly characterized as norm minimization (Razin & Cohen, 2020), though \mathcal{F}_1 norm minimization is a precise description under certain assumptions on the inputs (Boursier et al., 2022).

Compared to the body of work on inductive biases of single-task learning, theoretical treatments of MTL and PT+FT are more scarce. Some prior studies have characterized benefits of multi-task learning with a shared representational layer in terms of bounds on sample efficiency (Maurer et al., 2016; Wu et al., 2020). Others have characterized the learning dynamics of linear networks trained from nonrandom initializations, which can be applied to understand finetuning dynamics (Braun et al., 2022; Shachaf et al., 2021). However, while these works demonstrate an effect of pretrained initializations on learned solutions, the linear models they study do not capture the notion of feature learning we are interested in. A few empirical studies have compared the performance of multi-task learning vs. finetuning in language tasks, with mixed results depending on the task studied (Dery et al., 2021; Weller et al., 2022). Several authors have also observed that PT+FT outperforms PT + “linear probing” (training only the readout layer and keeping the previous layers frozen at their pretrained values), implying that finetuning benefits from the ability to learn task-specific features (Kumar et al., 2022; Kornblith et al., 2019b).

2.1 Inductive biases of diagonal linear networks

The theoretical component of our study relies heavily on a line of work (Woodworth et al., 2020; Pesme et al., 2021; Azulay et al., 2021; HaoChen et al., 2021; Moroshko et al., 2020) that studies the inductive bias of a simplified “diagonal linear network” model. Diagonal linear networks parameterize linear maps $f : \mathbb{R}^d \rightarrow \mathbb{R}$ as

$$f_{\vec{w}}(\vec{x}) = \vec{\beta}(\vec{w}) \cdot \vec{x}, \quad \beta_d(\vec{w}) := w_{+,d}^{(2)}w_{+,d}^{(1)} - w_{-,d}^{(2)}w_{-,d}^{(1)} \quad (1)$$

where $\vec{\beta}(\vec{w}) \in \mathbb{R}^D$. These correspond to two-layer linear networks in which the first layer consists of one-to-one connections, with duplicate + and - pathways to avoid saddle point dynamics around $\vec{w} = 0$. Woodworth et al. (2020) showed that overparameterized diagonal linear networks trained with gradient descent on mean squared error loss find the zero-training-error solution that minimizes $\|f\|_{\ell_2}^2 = \sum_{d=1}^D \beta_d^2$, when trained from large initialization (the “lazy” regime, equivalent to ridge regression). When trained from small initialization, networks instead minimize $\|f\|_{\ell_1} = \sum_{d=1}^D |\beta_d|$ (the “rich” regime). The latter ℓ_1 minimization bias is equivalent to minimizing the ℓ_2 norm of

the parameters \vec{w} (Appendix B). This bias is a linear analogue of feature-learning/feature-selection, as a model with an ℓ_1 penalty tends to learn solutions that depend on a sparse set of input dimensions.

3 Theory of PT+FT and MTL in diagonal linear networks

3.1 Finetuning combines rich and lazy learning

We now consider the behavior of PT+FT in overparameterized diagonal linear networks trained to minimize mean-squared error loss using gradient flow. We assume that all network weights are initialized prior to pre-training with a constant magnitude α . We further assume that during pretraining, network weights are optimized to convergence on the training dataset (X^{aux}, \vec{y}^{aux}) from the auxiliary task, then the second-layer weights ($w_{+,d}^{(2)}$ and $w_{-,d}^{(2)}$) are reinitialized with constant magnitude γ , and the network weights are further optimized to convergence on the main task dataset (X, \vec{y}) . The dynamics of the pretraining and finetuning steps can be derived as a corollary of the results of Woodworth et al. (2020) and Azulay et al. (2021):

Corollary 1. *If the gradient flow solution $\vec{\beta}^{aux}$ for the diagonal linear model in Eq. 1 during pretraining fits the auxiliary task training data with zero error (i.e. $X^{aux} \vec{\beta}^{aux} = \vec{y}^{aux}$), and following reinitialization of the second-layer weights and finetuning, the gradient flow solution $\vec{\beta}^*$ after finetuning fits the main task data with zero training error (i.e. $X \vec{\beta} = \vec{y}$), then*

$$\vec{\beta}^* = \arg \min_{\vec{\beta}} \|\vec{\beta}\|_Q \quad \text{s.t.} \quad X \vec{\beta} = \vec{y}, \quad (2)$$

$$\|\vec{\beta}\|_Q := \sum_{d=1}^D (|\beta_d^{aux}| + \gamma^2) q\left(\frac{2\beta_d}{|\beta_d^{aux}| + \gamma^2}\right), \quad q(z) = 2 - \sqrt{4 + z^2} + z \cdot \operatorname{arcsinh}(z/2). \quad (3)$$

It is informative to consider limits of the expression 3. As $\frac{|\beta_d|}{|\beta_d^{aux}| + \gamma^2} \rightarrow \infty$, the contribution of a feature d approaches $c|\beta_d|$ where $c \sim \mathcal{O}(\log(1/(|\beta_d^{aux}| + \gamma^2)))$. As $\frac{|\beta_d|}{|\beta_d^{aux}| + \gamma^2} \rightarrow 0$, the contribution converges to $\beta_d^2/|\beta_d^{aux}|$. Thus, for features that are weighted sufficiently strongly by the auxiliary task (large $|\beta_d^{aux}|$), finetuning minimizes a weighted ℓ_2 penalty that encourages reuse of features in proportion to their auxiliary task weight. For features specific to the auxiliary task (low $|\beta_d^{aux}|$), finetuning is biased to minimize an ℓ_1 penalty, encouraging sparsity in task-specific features. Overall, the penalty decreases with $|\beta_d^{aux}|$, encouraging feature reuse where possible. The combination of ℓ_1 and ℓ_2 behavior, as well as the dependence on $|\beta_d^{aux}|$, can be observed in Fig. 1a (left panel).

3.2 Multi-task training learns sparse and shared features

Now we consider MTL for diagonal linear networks. A multi-output diagonal linear network with O outputs can be written as

$$f_{\vec{w}}(\vec{x}) = \beta(\vec{w})\vec{x}, \quad \vec{\beta}_o(\vec{w}) := \vec{w}_{+,o}^{(2)} \circ \vec{w}_+^{(1)} - \vec{w}_{-,o}^{(2)} \circ \vec{w}_-^{(1)} \quad (4)$$

where $\beta(\vec{w}) \in \mathbb{R}^{O \times D}$, and \circ is elementwise multiplication. We consider the effect of minimizing $\|\vec{w}\|_2$, as an approximation of the inductive bias of training a network from small initialization. We argue that $\|\vec{w}\|_2$ minimization is a reasonable heuristic. First, the analogous result holds in the single-output case for infinitesimally small initialization and two layers (though not for deeper networks, see Woodworth et al. (2020)). Second, for cross-entropy loss it has been shown that gradient flow converges to a KKT point of a max-margin/min-parameter-norm objective (Lyu & Li, 2020). Finally, explicit ℓ_2 parameter norm regularization (“weight decay”) is commonly used.

In MTL, a result of Dai et al. (2021) shows that a parameter norm minimization bias translates to minimizing an $\ell_{1,2}$ penalty that incentivizes group sparsity (Yuan & Lin, 2006) on the learned linear map β : $\|\beta\|_{1,2} := 2 \sum_{d=1}^D \|\vec{\beta}_{\cdot,d}\|_2$ (a self-contained proof is given in Appendix B). For the specific case of two outputs corresponding to main (first index) and auxiliary (second index) tasks, we have:

Corollary 2. *Using the multi-output diagonal linear model of Eq. 4 with two outputs, adopting shorthand notation $\vec{\beta} := \vec{\beta}_1$, $\vec{\beta}^{aux} := \vec{\beta}_2$, a solution β^* with minimal parameter norm $\|\vec{w}_+^{(1)}\|_2^2 + \|\vec{w}_-^{(1)}\|_2^2 + \sum_o \|\vec{w}_{+,o}^{(2)}\|_2^2 + \sum_o \|\vec{w}_{-,o}^{(2)}\|_2^2$ subject to the constraint that it fits the training data ($X \vec{\beta} = \vec{y}$, $X^{aux} \vec{\beta}^{aux} = \vec{y}^{aux}$) also minimizes the following:*

$$\beta^* = \arg \min_{\beta} \left(2 \sum_{d=1}^D \sqrt{(\beta_d^{aux})^2 + (\beta_d)^2} \right) \quad \text{s.t.} \quad X \vec{\beta} = \vec{y}, \quad X^{aux} \vec{\beta}^{aux} = \vec{y}^{aux}. \quad (5)$$

This penalty (plotted in Fig. 1a, right panel), encourages using shared features for the main and auxiliary tasks, as the contribution of β_d to the square-root expression is smaller when β_d^{aux} is large. As $\frac{|\beta_d|}{|\beta_d^{aux}|+\gamma^2} \rightarrow \infty$, the penalty converges to $2|\beta_d|$, a sparsity-inducing ℓ_1 bias for task-specific features. As $\frac{|\beta_d|}{|\beta_d^{aux}|+\gamma^2} \rightarrow 0$ it converges to $\frac{\beta_d^2}{|\beta_d^{aux}|}$, a weighted ℓ_2 bias as in the PT+FT case.

3.3 Comparison of the MTL and PT+FT biases

We now compare the MTL and PT+FT penalties given above.¹ The MTL and PT+FT penalties have many similarities. Both decrease as $|\beta_d^{aux}|$ increases, both are proportional to $|\beta_d|$ as $\frac{|\beta_d|}{|\beta_d^{aux}|+\gamma^2} \rightarrow \infty$, and both are proportional to $\frac{\beta_d^2}{|\beta_d^{aux}|}$ as $\frac{|\beta_d|}{|\beta_d^{aux}|+\gamma^2} \rightarrow 0$. These similarities are evident in Fig. 1a. However, two differences between the penalties merit attention.

First, the relative weights of the ℓ_1 and weighted ℓ_2 penalties are different between MTL and PT+FT. In particular, in the ℓ_1 penalty limit, there is an extra factor of order $\mathcal{O}(\log(1/(|\beta_d^{aux}| + \gamma^2)))$ in the PT+FT penalty. Assuming small initializations, this factor tends to be larger than 2, the corresponding coefficient in the MTL penalty. Thus, PT+FT is more strongly biased toward reusing features from the auxiliary task (i.e. features where $\beta_d^{aux} \gg 0$) compared to MTL. We are careful to note, however, that in the case of nonlinear networks this effect is complicated by a qualitatively different phenomenon with effects in the reverse direction (see Section 5.2).

Second, the two norms behave differently for intermediate values of $\frac{\beta_d}{|\beta_d^{aux}|}$. In particular, as β_d increases beyond the value of β_d^{aux} , the MTL norm quickly grows insensitive to the value of β_d^{aux} (Fig. 1a, right panel). On the other hand, the PT+FT penalty remains sensitive to the value of β_d^{aux} even for fairly large values of β_d , well into the ℓ_1 -like penalty regime (Fig. 1a, left panel). This property of the PT+FT norm, in theory, can enable finetuned networks to exhibit a rich regime-like sparsity bias while remaining influenced by their initializations. We explore this effect in section 4.2.

4 Verification and implications of the linear theory

To validate these theoretical characterizations and illustrate their consequences, we performed experiments with diagonal linear networks in a teacher-student setup. We consider linear regression tasks defined by $\vec{w} \in \mathbb{R}^{1000}$ with a sparse set of k non-zero entries. We sample two such vectors, corresponding to ‘‘auxiliary’’ and ‘‘main’’ tasks, varying the number of nonzero entries k_{aux} and k_{main} , and the number of shared features (overlapping nonzero entries). We train diagonal linear networks on data generated from these ground-truth weights, using 1024 auxiliary task samples and varying the number of main task samples. For re-initialization of the readout, we use $\gamma = 10^{-3}$.

4.1 Feature reuse and sparse task-specific feature selection in PT+FT and MTL

We begin with tasks in which $k_{aux} = k_{main} = 40$ (both tasks use the same number of features), varying the overlap between the feature sets (Fig. 1b). Both MTL and PT+FT display greater sample efficiency than single-task learning when the feature sets overlap. This behavior is consistent with an inductive bias towards feature sharing. Additionally, both MTL and PT+FT substantially outperform single-task lazy-regime learning, and nearly match single-task rich-regime learning, when the feature sets are disjoint. This is consistent with the ℓ_1 -like biases for task-specific features derived above, which coincide with the bias of single-task rich-regime (but not lazy-regime) learning. When the tasks partially overlap, MTL and PT+FT outperform both single-task learning and a PT + linear probing strategy (finetuning only the second-layer weights $w_{+,d}^{(2)}$ and $w_{-,d}^{(2)}$), which by construction cannot implement the kind of task-specific feature selection that MTL and PT+FT implement. Thus, both PT+FT and MTL are capable of simultaneously exhibiting a feature sharing bias while also displaying task-specific feature selection, consistent with the hybrid $\ell_1 /$ weighted- ℓ_2 regularization penalties derived above. Interestingly, PT+FT performs better than MTL when the tasks use identical feature sets. This behavior is consistent with the Q -norm more strongly penalizing new-feature learning than the MTL norm, as observed in Section 3.3.

To more directly test for a bias toward sparsity in task-specific features, we computed the fraction of overall weight norm in the learned main task linear predictor $\vec{\beta}$ that is captured by the top k strongest weights. We confirmed that the learned linear maps are indeed effectively sparse for both MTL and PT+FT, even when the main and auxiliary tasks contain distinct features and few samples are available (Fig. 1c for 30/40 overlap case, see Appendix E, Fig. 5e for full

¹We note that it is not a strict apples-to-apples comparison as the PT+FT penalty describes the bias of gradient flow, while the given MTL penalty describes the bias of $\|\vec{w}\|_2$ minimization.

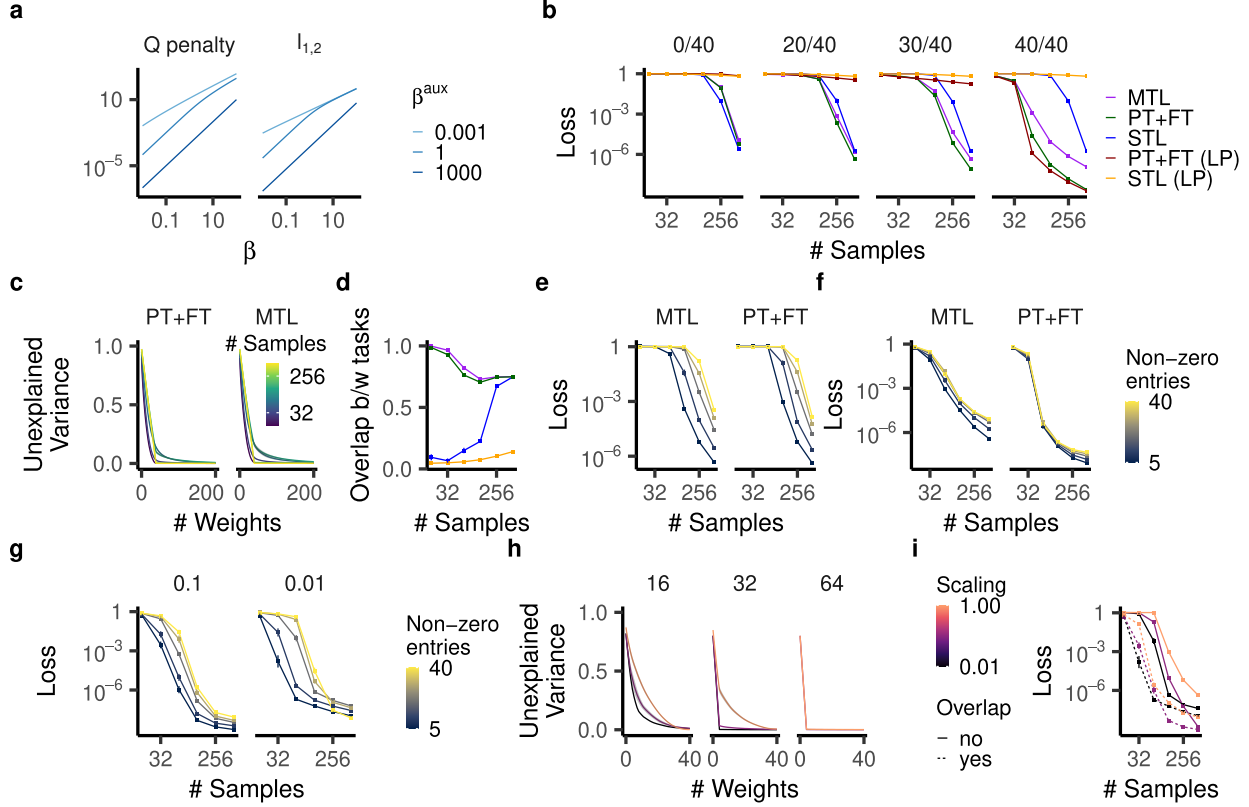


Figure 1: Diagonal linear networks. **a**: Q (Eq. 3) and $\ell_{1,2}$ (Eq. 5) penalties, assuming negligible γ for the Q penalty. Log scale on both axes. **b**: Main task generalization loss for networks trained with MTL, PT+FT, single-task learning (STL), PT + finetuning via linear probing (PT+FT (LP)), and single-task linear probing (STL (LP), equivalent to lazy single-task learning, or ridge regression). Log scale on both axes. **c**: Proportion of variance concentrated in the top k weights, as a function of k (for an overlap of 30/40). The rapid decrease demonstrates the sparsity of the learned solution. **d**: Proportion of weight norm in the 40 dimensions relevant for the auxiliary task (again for an overlap of 30/40). **e**: Generalization loss for case in which auxiliary task (40 nonzero ground-truth weights) and main task (number of ground-truth weights indicated by color scale) share no common features. **f**: Generalization loss for case in which main task uses a subset of the features used by the auxiliary task. **g**: Same as PT+FT case in panel **e**, but with the network weights rescaled by 0.1 or 0.01 (panel title) following pretraining. A sparsity bias is evident, unlike in **e** (rescaling = 1.0 case), and more pronounced as rescaling coefficient decreases. **h**: Unexplained variance as a function of weight scaling. On low numbers of samples, low scalings result in much more pronounced sparsity. **i**: Performance in the case of 5 main task features chosen either as a subset of the auxiliary task features (“shared”) or disjoint from them (“task-specific”), varying the rescaling of weights following pretraining (1, 0.1, and 0.01). A bias toward feature reuse is evident even at the low scalings, which yield a sparsity bias (panels **g**, **h**).

suite of experiments)². Further, to test for a bias toward feature sharing, we computed the fraction of the norm of $\vec{\beta}$ captured by the 40 features learned on the main task (Fig. 1d, see Appendix E, Fig. 5f for full suite of experiments). For MTL and PT+FT, this fraction is high for very few samples (indicating an inductive bias toward feature sharing) and gradually approaches the true overlap (30/40=0.75). Finally, we also directly measured the $\ell_{1,2}$ and Q norms of the solutions learned by networks (Appendix E, Fig. 5a), confirming a bias toward minimization of these norms in MTL and PT+FT, respectively.

As another test of the predicted bias toward sparsity in task-specific features, we conducted experiments in which the main and auxiliary task features do not overlap, and varied the number k_{main} of main task features. We find that both MTL and PT+FT are more sample-efficient when the main task is sparser, consistent with the prediction (Fig. 1e).

²Note that there is a slight non-monotonicity in learned solution sparsity as a function of number of main task samples; this is because of the discrepancy of L1 norm minimization and L0 “norm” minimization (sparsity maximization), see Appendix E Fig. 5c,d

4.2 PT+FT exhibits a scaling-dependent nested feature-selection regime

In the limit of small $\frac{|\beta_d|}{|\beta_d^{aux}|}$, both the MTL and PT+FT penalties converge to weighted ℓ_2 norms. Notably, the behavior is ℓ_2 -like even when $\frac{|\beta_d|}{|\beta_d^{aux}|} \approx 1$ (Fig. 1a). Thus, among features that are weighted as strongly in the auxiliary task as the main task, the theory predicts that PT+FT and MTL should exhibit no sparsity bias. To test this, we use a teacher-student setting in which all the main task features are a subset of the auxiliary task features, i.e. $k_{main} \leq k_{aux}$, and the number of overlapping units is equal to k_{main} . We find that MTL and PT+FT derive little to no sample efficiency benefit from sparsity in this context, consistent with an ℓ_2 -like minimization bias (Fig. 1f).

However, as remarked in Section 3.3, in the regime where $\frac{|\beta_d|}{|\beta_d^{aux}|}$ is greater than 1 but not astronomically large, the PT+FT penalty maintains an inverse dependence on $|\beta_d^{aux}|$ while exhibiting approximately ℓ_1 scaling. In this regime, we would expect PT+FT to be adept at efficiently learning the tasks just considered, which require layering a bias toward sparse solutions on top of a bias toward features learned during pretraining. We can produce this behavior in these tasks by rescaling the weights of the network following pretraining by a factor less than 1. In line with the prediction of the theory, performing this manipulation enables PT+FT to leverage sparse structure *within* auxiliary task features (Fig. 1g). We confirm that weight rescaling does in fact lead to extraction of a sparse set of features by analyzing, as in Fig. 1c, the extent to which the learned linear predictor on the main task is concentrated on a small set of features (Fig. 1h). We also confirm that networks in the nested feature selection regime retain their ability to privilege features learned during pretraining above others (Fig. 1i), and that this phenomenon results from a bias toward feature reuse that grows less strong as the weight rescaling factor is decreased (Appendix 5, Fig. 5b).

This (initialization-dependent, ℓ_1 -minimizing) behavior is qualitatively distinct from the (initialization-dependent, weighted ℓ_2 -minimizing) lazy regime and the (initialization-independent, ℓ_1 -minimizing) feature-learning regimes. We refer to it as the *nested feature-selection* regime. This inductive bias may be useful when pretraining tasks are more general or complex (and thus involve more features) than the target task. This situation may be common in practice, as networks are often pre-trained on general-purpose tasks before finetuning for more specific applications.

5 Nonlinear networks

5.1 Similarities to linear models: feature reuse and sparse feature learning

We now examine the extent to which our findings above apply to nonlinear models, focusing on single hidden-layer ReLU networks. We find that, as in the diagonal linear case, MTL and PT+FT effectively leverage feature reuse (outperforming single-task learning when tasks share features, Fig. 2a, right) and perform effective feature learning of task-specific features (nearly matching rich single-task learning and substantially outperforming lazy single-task learning when task features are not shared, Fig. 2a, left panel). Moreover, as in the linear theory, both effects can be exhibited simultaneously (Fig. 2a, middle panels). We also confirm that task-specific feature learning exhibits a sparsity bias (greater sample efficiency when non-shared main task features are sparse, Fig. 2b).

We corroborate these claims by analyzing the sparsity of the learned solutions. We perform k-means clustering with K clusters on the normalized input weights to each hidden-layer neuron in a network. We measure the extent to which K cluster centers are able to explain the variance in input weights across hidden units; the fraction of variance left unexplained is commonly referred to as the “inertia.” For values of K at which the inertia is close to zero, we can say that (to a good approximation) the network effectively makes use of at most K features. We find that the solutions learned by PT+FT and MTL are indeed quite sparse (comparable to the sparsity of solutions learned by single-task learning), even when the auxiliary task and main task features are disjoint (see Fig. 2c for representative example, and Appendix E, Fig. 6c,d for full suite of experiments), supporting the claim that PT+FT and MTL are biased toward sparsity in task-specific features. Further, the features learned by PT+FT and MTL are more aligned with the ground truth features than those learned by STL (Fig. 2d, see Appendix E, Fig. 6e for full suite of experiments), supporting the claim that PT+FT and MTL are biased toward sharing main and auxiliary task features.

5.2 PT+FT bias extends to features correlated with auxiliary task features

Interestingly, in cases with shared features between tasks, we find that finetuning can underperform multi-task learning (Fig. 2a), in contrast to the diagonal linear case. We hypothesize that this effect is caused by the fact that during finetuning, hidden units may not only change their magnitudes, but also the directions $\vec{\theta}_h$ of their input weights. Thus, in nonlinear networks, PT+FT may not strictly exhibit a bias toward reusing features across tasks, but rather a “softer” bias that also privileges features correlated with (but not identical to) those learned during pretraining. To test this hypothesis, we conduct experiments in which the ground-truth auxiliary and main tasks rely on correlated but distinct

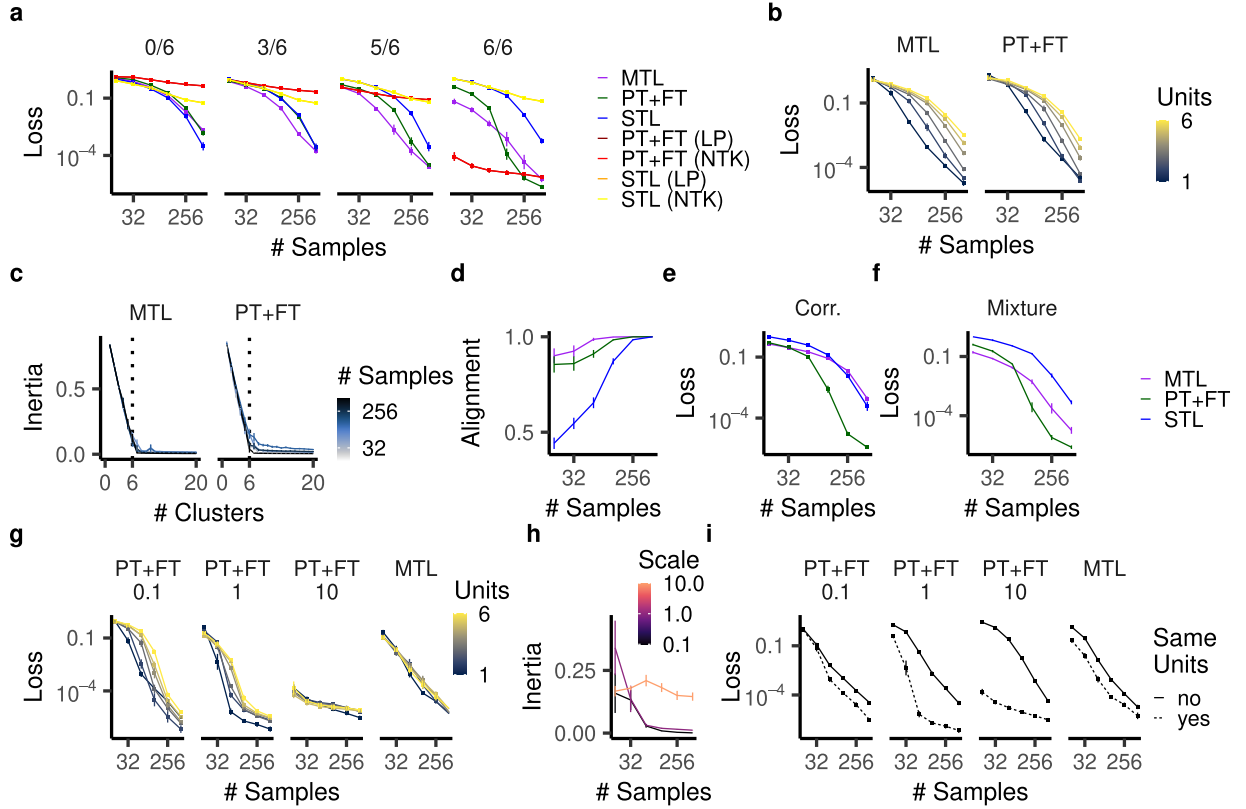


Figure 2: Nonlinear networks. **a**: Generalization loss (log-scaled) for different numbers of overlapping features (out of 6 total) between main and auxiliary tasks. NTK indicates the (lazy) tangent kernel solution. **b**: Generalization loss as a function of number of main task features (units in teacher network) in tasks where main and auxiliary task features are disjoint. **c**: Inertia (unexplained variance) for different numbers of clusters (overlap 5/6 case). The rapid decrease demonstrates the feature sparsity of learned solutions for both MTL and PT+FT. **d**: Alignment between main task features and the best matching input-weight cluster found by k-means with $K=12$ (the total number of features for both tasks). The high alignment for PT+FT and MTL compared to STL demonstrates a bias toward feature sharing. **e**: Generalization loss in tasks where main-task features are correlated (0.9 cosine similarity of input weights) with corresponding auxiliary task features. **f**: Generalization loss for an example with both identically shared and correlated features between tasks. **g**: Generalization loss for PT+FT using different rescalings of network weights following pretraining (0.1, 1, and 10.0), and also for MTL, on tasks in which main task features are a subset of auxiliary task features. Color indicates number of main task features. **h**: Inertia for k-means clustering with a single cluster ($K=1$) for networks finetuned on a task with a single main task feature chosen from one of the auxiliary task features. Low inertia demonstrates that the network indeed learns a sparse solution. **i**: Generalization loss for same strategies as in panel g, on tasks in which main task features are either a subset of auxiliary task features (“shared”) or disjoint (“task-specific”).

features. Indeed, we find PT+FT outperforms MTL in this case (Fig. 2e). Thus, PT+FT (compared to MTL) trades off the flexibility to “softly” share features for reduced sample-efficiency when such flexibility is not needed. In Appendix E, Fig. 6e we show that MTL learns features that are more aligned with the ground-truth task features than PT+FT when main and auxiliary task features are identically shared, but the reverse is true when main and auxiliary task features are merely correlated.

In realistic settings, the degree of correlation between features across tasks is likely heterogeneous. To simulate such a scenario, we experiment with auxiliary and main tasks with a mixture of identically shared and correlated features. In this setting, we find that MTL outperforms PT+FT for fewer main task samples, while PT+FT outperforms MTL when more samples are available (Fig. 2f). We hypothesize that this effect arises because the flexibility of PT+FT to rotate hidden unit inputs is most detrimental in the few-sample regime where there is insufficient data to identify correct features.

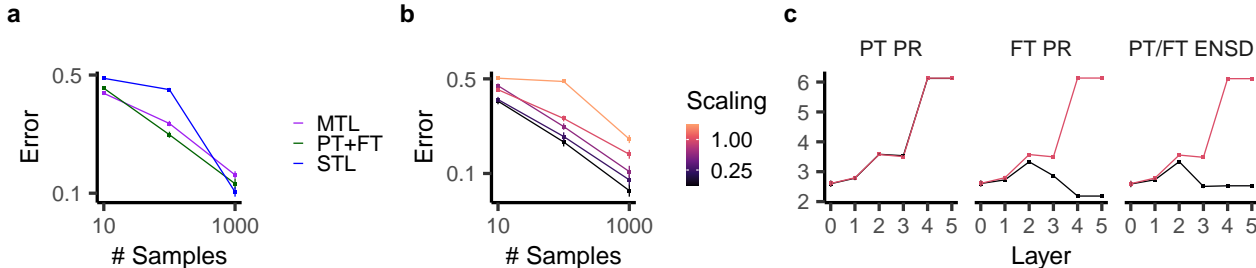


Figure 3: **a**: Test error on CIFAR-100 experiment as a function of main task samples (log scale on both axes). **b**: Test error on CIFAR-100 for PT+FT with different weight rescaling values following pretraining. **c**: Participation ratio (PR; measuring dimensionality) of the pretrained and finetuned networks and the effective number of shared dimensions (ENSD) between them.

5.3 The nested feature-selection regime

In Section 4.2, we uncovered a “nested feature-selection” regime, obtained at intermediate values of $\frac{|\beta_d|}{|\beta_d^{aux}|}$ between the rich and lazy regimes, in which PT+FT is biased toward sparse feature selection among the features learned during pretraining. To test whether the same phenomenon arises in ReLU networks, we rescale the network weights following pretraining by various factors (which has the effect of scaling $|\beta_d^{aux}|$ for all d). We evaluate performance on a suite of tasks that vary the number of features in the main task teacher network and whether those features are shared with the auxiliary task. At intermediate rescaling values we confirm the presence of a nested feature selection regime, characterized by a bias toward sparsity among features reused from the auxiliary task (Fig. 2g) and a preference for reusing features over task-specific feature learning (Fig. 2i) which arises from a bias toward reusing auxiliary task features (Appendix E, Fig. 6g). Further rescaling in either direction uncovers the initialization-insensitive rich / feature-learning regime and the initialization-biased lazy learning regime. As predicted by the linear theory, we do not observe nested feature selection behavior in MTL. Note that for different tasks and architectures, different rescaling values may be needed to enter the nested feature learning regime.

To shed further light on this regime, we analyzed the effective sparsity of learned solutions using the k-means clustering approach introduced previously. We find that networks identified above as in the nested feature selection regime indeed learn sparse (effectively 1-feature) solutions when the main task consists of a single auxiliary task feature (Fig. 2h). By contrast, networks with weights rescaled by a factor of 10.0 following pretraining exhibit no such nested sparsity bias (consistent with lazy-regime behavior). Additionally, supporting the idea that the nested feature selection regime maintains a bias toward feature reuse (Fig. 1i, Fig. 2i), we find that networks in this regime exhibit higher alignment of learned features with the ground-truth teacher network when the main task features are a subset of the auxiliary task features, compared to when they are disjoint from the auxiliary task features (Appendix E, Fig. 6g). This alignment benefit is mostly lost when networks are rescaled by a factor of 0.1 following pretraining (a signature of rich-regime behavior).

6 Practical applications to deep networks and real datasets

Our analysis has focused on shallow networks trained on synthetic tasks. To test the applicability of our insights, we conduct experiments with convolutional networks (ResNet-18) on a vision task (CIFAR-100), using classification of two image categories (randomly sampled for each training run) as the primary task and classification of the other 98 as the auxiliary task. As in our experiments above, MTL and PT+FT improve sample efficiency compared to single-task learning (Fig. 3a). Moreover, the results corroborate our findings in Section 5.2 that MTL performs better than PT+FT with fewer main task samples, while the reverse is true with more samples. A similar finding was made by Weller et al. (2022) in natural language processing tasks.

Our findings in Section 4.2 and Section 5.3 indicate that the nested feature selection bias of PT+FT can be exposed or masked by rescaling the network weights following pretraining. Such a bias may be beneficial when the main task depends on a small subset of features learned during pretraining, as may often be the case in practice. We experiment with rescaling in our CIFAR setup. We find that rescaling values less than 1 improve finetuning performance (Fig. 3b). These results suggest that rescaling network weights before finetuning may be practically useful. We corroborate this hypothesis with additional experiments using networks pre-trained on ImageNet (see Appendix F).

To facilitate comparison of the phenomenology in deep networks with our teacher-student experiments above, we propose a signature of nested feature selection that can be characterized without knowledge of the underlying feature space. Specifically, we propose to measure (1) the *dimensionality* of the network representation pre- and post-finetuning, and (2) the extent to which the representational structure post-finetuning is shared with / inherited from that of the network following pretraining prior to finetuning. We employ the commonly used *participation ratio* (PR; Gao et al., 2017) as a measure of dimensionality, and the *effective number of shared dimensions* (ENSD, Giaffar et al. 2023) as a soft measure of the number of aligned principal components between two representations. Intuitively, the PR and ENSD of network representations pre- and post-finetuning capture the key phenomena of the nested feature selection regime: we expect the dimensionality of network after finetuning to be lower than after pretraining ($PR(\mathbf{X}_{FT}) < PR(\mathbf{X}_{PT})$), and for nearly all of the representational dimensions expressed by the network post-finetuning to be inherited from the network state after pretraining ($ENSD(\mathbf{X}_{PT}, \mathbf{X}_{FT}) \approx PR(\mathbf{X}_{FT})$). We validate that this description holds in our nonlinear teacher-student experiments with networks in the nested feature selection regime (Appendix G, Fig. 8c). Moreover, we find that the ResNet-18 model with rescaling applied (but not without rescaling) exhibits the same phenomenology (Fig. 3c). This supports the hypothesis that the observed benefits of rescaling indeed arise from pushing the network into the nested feature selection regime (see Appendix G for more details).

7 Conclusion

In this work we have provided a detailed characterization of the inductive biases associated with two common training strategies, MTL and PT+FT. We find that these biases incentivize a combination of feature sharing and sparse task-specific feature learning. In the case of PT+FT, we characterized a novel learning regime – the nested feature-selection regime – which encourages sparsity *within* features inherited from pretraining. This insight motivates simple techniques for improving PT+FT performance by pushing networks into this regime, which shows promising empirical results. We also identified another distinction between PT+FT and MTL – the ability to use “soft” feature sharing – that leads to a tradeoff in their relative performance as a function of dataset size.

More work is needed to test these phenomena in more complex tasks and larger models. There are also promising avenues for extending our theoretical work. First, in this paper we did not analytically describe the dynamics of PT+FT in ReLU networks, but we expect more progress could be made on this front. Second, our diagonal linear theory could be extended to the case of the widely used cross-entropy loss (see Appendix C for comments on this point). Third, we believe it is important to extend this theoretical framework to more complex network architectures. Nevertheless, our present work already provides new and practical insights into the function of auxiliary task learning.

References

- Azulay, S., Moroshko, E., Nacson, M. S., Woodworth, B. E., Srebro, N., Globerson, A., and Soudry, D. On the Implicit Bias of Initialization Shape: Beyond Infinitesimal Mirror Descent. In *Proceedings of the 38th International Conference on Machine Learning*, pp. 468–477. PMLR, July 2021. URL <https://proceedings.mlr.press/v139/azulay21a.html>.
- Bommasani, R., Hudson, D. A., Adeli, E., Altman, R., Arora, S., von Arx, S., Bernstein, M. S., Bohg, J., Bosselut, A., Brunskill, E., Brynjolfsson, E., Buch, S., Card, D., Castellon, R., Chatterji, N., Chen, A., Creel, K., Davis, J. Q., Demszky, D., Donahue, C., Doumbouya, M., Durmus, E., Ermon, S., Etchemendy, J., Ethayarajh, K., Fei-Fei, L., Finn, C., Gale, T., Gillespie, L., Goel, K., Goodman, N., Grossman, S., Guha, N., Hashimoto, T., Henderson, P., Hewitt, J., Ho, D. E., Hong, J., Hsu, K., Huang, J., Icard, T., Jain, S., Jurafsky, D., Kalluri, P., Karamcheti, S., Keeling, G., Khani, F., Khattab, O., Koh, P. W., Krass, M., Krishna, R., Kuditipudi, R., Kumar, A., Ladhak, F., Lee, M., Lee, T., Leskovec, J., Levent, I., Li, X. L., Li, X., Ma, T., Malik, A., Manning, C. D., Mirchandani, S., Mitchell, E., Munyikwa, Z., Nair, S., Narayan, A., Narayanan, D., Newman, B., Nie, A., Niebles, J. C., Nilforoshan, H., Nyarko, J., Ogut, G., Orr, L., Papadimitriou, I., Park, J. S., Piech, C., Portelance, E., Potts, C., Raghunathan, A., Reich, R., Ren, H., Rong, F., Roohani, Y., Ruiz, C., Ryan, J., Ré, C., Sadigh, D., Sagawa, S., Santhanam, K., Shih, A., Srinivasan, K., Tamkin, A., Taori, R., Thomas, A. W., Tramèr, F., Wang, R. E., Wang, W., Wu, B., Wu, J., Wu, Y., Xie, S. M., Yasunaga, M., You, J., Zaharia, M., Zhang, M., Zhang, T., Zhang, X., Zhang, Y., Zheng, L., Zhou, K., and Liang, P. On the Opportunities and Risks of Foundation Models, July 2022. URL <http://arxiv.org/abs/2108.07258>. arXiv:2108.07258 [cs].
- Boursier, E., Pillaud-Vivien, L., and Flammarion, N. Gradient flow dynamics of shallow ReLU networks for square loss and orthogonal inputs. May 2022. URL <https://openreview.net/forum?id=L74c-iUxQ1I>.
- Braun, L., Dominé, C., Fitzgerald, J., and Saxe, A. Exact learning dynamics of deep linear networks with prior knowledge. *Advances in Neural Information Processing Systems*, 35:6615–

- 6629, December 2022. URL https://proceedings.neurips.cc/paper_files/paper/2022/hash/2b3bb2c95195130977a51b3bb251c40a-Abstract-Conference.html.
- Chizat, L. and Bach, F. Implicit Bias of Gradient Descent for Wide Two-layer Neural Networks Trained with the Logistic Loss. In *Proceedings of Thirty Third Conference on Learning Theory*, pp. 1305–1338. PMLR, July 2020. URL <https://proceedings.mlr.press/v125/chizat20a.html>. ISSN: 2640-3498.
- Dai, Z., Karzand, M., and Srebro, N. Representation Costs of Linear Neural Networks: Analysis and Design. In *Advances in Neural Information Processing Systems*, volume 34, pp. 26884–26896. Curran Associates, Inc., 2021. URL https://proceedings.neurips.cc/paper_files/paper/2021/hash/e22cb9d6bbb4c290a94e4fff4d68a831-Abstract.html.
- Dery, L. M., Michel, P., Talwalkar, A., and Neubig, G. Should We Be Pre-training? An Argument for End-task Aware Training as an Alternative. October 2021. URL <https://openreview.net/forum?id=2b02x8NAIMB>.
- Du, Y., Liu, Z., Li, J., and Zhao, W. X. A Survey of Vision-Language Pre-Trained Models, July 2022. URL <http://arxiv.org/abs/2202.10936>. arXiv:2202.10936 [cs].
- Gao, P., Trautmann, E., Yu, B., Santhanam, G., Ryu, S., Shenoy, K., and Ganguli, S. A theory of multineuronal dimensionality, dynamics and measurement, November 2017. URL <https://www.biorxiv.org/content/10.1101/214262v2>.
- Giaffar, H., Buxó, C. R., and Aoi, M. The effective number of shared dimensions: A simple method for revealing shared structure between datasets, July 2023. URL <https://www.biorxiv.org/content/10.1101/2023.07.27.550815v1>.
- Gunasekar, S., Lee, J. D., Soudry, D., and Srebro, N. Implicit Bias of Gradient Descent on Linear Convolutional Networks. In *Advances in Neural Information Processing Systems*, volume 31. Curran Associates, Inc., 2018. URL <https://proceedings.neurips.cc/paper/2018/hash/0e98aeeb54acf612b9eb4e48a269814c-Abstract.html>.
- HaoChen, J. Z., Wei, C., Lee, J., and Ma, T. Shape Matters: Understanding the Implicit Bias of the Noise Covariance. In *Proceedings of Thirty Fourth Conference on Learning Theory*, pp. 2315–2357. PMLR, July 2021. URL <https://proceedings.mlr.press/v134/haochen21a.html>.
- Huh, M., Mobahi, H., Zhang, R., Cheung, B., Agrawal, P., and Isola, P. The Low-Rank Simplicity Bias in Deep Networks, March 2023. URL <http://arxiv.org/abs/2103.10427>. arXiv:2103.10427 [cs].
- Jaderberg, M., Mnih, V., Czarnecki, W. M., Schaul, T., Leibo, J. Z., Silver, D., and Kavukcuoglu, K. Reinforcement Learning with Unsupervised Auxiliary Tasks, November 2016. URL <http://arxiv.org/abs/1611.05397>. arXiv:1611.05397 [cs].
- Kornblith, S., Norouzi, M., Lee, H., and Hinton, G. Similarity of Neural Network Representations Revisited. In *Proceedings of the 36th International Conference on Machine Learning*, pp. 3519–3529. PMLR, May 2019a. URL <https://proceedings.mlr.press/v97/kornblith19a.html>.
- Kornblith, S., Shlens, J., and Le, Q. V. Do better ImageNet models transfer better? 2019b. URL <https://arxiv.org/pdf/1805.08974.pdf>.
- Kumar, A., Raghunathan, A., Jones, R., Ma, T., and Liang, P. Fine-Tuning can Distort Pretrained Features and Underperform Out-of-Distribution, February 2022. URL <http://arxiv.org/abs/2202.10054>. arXiv:2202.10054 [cs].
- Lyu, K. and Li, J. Gradient Descent Maximizes the Margin of Homogeneous Neural Networks, December 2020. URL <http://arxiv.org/abs/1906.05890>. arXiv:1906.05890 [cs, stat].
- Maurer, A., Pontil, M., and Romera-Paredes, B. The Benefit of Multitask Representation Learning. *Journal of Machine Learning Research*, 17(81):1–32, 2016. ISSN 1533-7928. URL <http://jmlr.org/papers/v17/15-242.html>.
- Moroshko, E., Woodworth, B. E., Gunasekar, S., Lee, J. D., Srebro, N., and Soudry, D. Implicit Bias in Deep Linear Classification: Initialization Scale vs Training Accuracy. In *Advances in Neural Information Processing Systems*, volume 33, pp. 22182–22193. Curran Associates, Inc., 2020. URL <https://proceedings.neurips.cc/paper/2020/hash/fc2022c89b61c76bbef978f1370660bf-Abstract.html>.
- Mulayoff, R., Michaeli, T., and Soudry, D. The Implicit Bias of Minima Stability: A View from Function Space. In *Advances in Neural Information Processing Systems*, volume 34, pp. 17749–17761. Curran Associates, Inc., 2021. URL <https://proceedings.neurips.cc/paper/2021/hash/944a5ae3483ed5c1e10bbccb7942a279-Abstract.html>.

- Nacson, M. S., Gunasekar, S., Lee, J., Srebro, N., and Soudry, D. Lexicographic and Depth-Sensitive Margins in Homogeneous and Non-Homogeneous Deep Models. In *Proceedings of the 36th International Conference on Machine Learning*, pp. 4683–4692. PMLR, May 2019. URL <https://proceedings.mlr.press/v97/nacson19a.html>. ISSN: 2640-3498.
- Neyshabur, B. Implicit Regularization in Deep Learning, September 2017. URL <http://arxiv.org/abs/1709.01953>. arXiv:1709.01953 [cs].
- Pesme, S., Pillaud-Vivien, L., and Flammarion, N. Implicit Bias of SGD for Diagonal Linear Networks: a Provable Benefit of Stochasticity. November 2021. URL <https://openreview.net/forum?id=vvi7KqHQiA>.
- Rahaman, N., Baratin, A., Arpit, D., Draxler, F., Lin, M., Hamprecht, F., Bengio, Y., and Courville, A. On the Spectral Bias of Neural Networks. September 2018. URL <https://openreview.net/forum?id=r1gR2sC9FX>.
- Razin, N. and Cohen, N. Implicit Regularization in Deep Learning May Not Be Explainable by Norms. In *Advances in Neural Information Processing Systems*, volume 33, pp. 21174–21187. Curran Associates, Inc., 2020. URL <https://proceedings.neurips.cc/paper/2020/hash/f21e255f89e0f258accbe4e984eef486-Abstract.html>.
- Refinetti, M., Ingrosso, A., and Goldt, S. Neural networks trained with SGD learn distributions of increasing complexity, May 2023. URL <http://arxiv.org/abs/2211.11567>. arXiv:2211.11567 [cond-mat, stat].
- Savarese, P., Evron, I., Soudry, D., and Srebro, N. How do infinite width bounded norm networks look in function space?: 32nd Conference on Learning Theory, COLT 2019. *Proceedings of Machine Learning Research*, 99:2667–2690, 2019. URL <http://www.scopus.com/inward/record.url?scp=85132757852&partnerID=8YFLogxK>.
- Shachaf, G., Brutzkus, A., and Globerson, A. A Theoretical Analysis of Fine-tuning with Linear Teachers. In *Advances in Neural Information Processing Systems*, volume 34, pp. 15382–15394. Curran Associates, Inc., 2021. URL <https://proceedings.neurips.cc/paper/2021/hash/82039d16dce0aab3913b6a7ac73deff7-Abstract.html>.
- Steed, R., Panda, S., Kobren, A., and Wick, M. Upstream Mitigation Is Not All You Need: Testing the Bias Transfer Hypothesis in Pre-Trained Language Models. In *Proceedings of the 60th Annual Meeting of the Association for Computational Linguistics (Volume 1: Long Papers)*, pp. 3524–3542, Dublin, Ireland, May 2022. Association for Computational Linguistics. doi: 10.18653/v1/2022.acl-long.247. URL <https://aclanthology.org/2022.acl-long.247>.
- Vafaeikia, P., Namdar, K., and Khalvati, F. A Brief Review of Deep Multi-task Learning and Auxiliary Task Learning, July 2020. URL <http://arxiv.org/abs/2007.01126>. arXiv:2007.01126 [cs, stat].
- Wang, A. and Russakovsky, O. Overwriting Pretrained Bias with Finetuning Data, August 2023. URL <http://arxiv.org/abs/2303.06167>. arXiv:2303.06167 [cs].
- Weller, O., Seppi, K., and Gardner, M. When to Use Multi-Task Learning vs Intermediate Fine-Tuning for Pre-Trained Encoder Transfer Learning. In *Proceedings of the 60th Annual Meeting of the Association for Computational Linguistics (Volume 2: Short Papers)*, pp. 272–282, Dublin, Ireland, May 2022. Association for Computational Linguistics. doi: 10.18653/v1/2022.acl-short.30. URL <https://aclanthology.org/2022.acl-short.30>.
- Woodworth, B., Gunasekar, S., Lee, J. D., Moroshko, E., Savarese, P., Golan, I., Soudry, D., and Srebro, N. Kernel and Rich Regimes in Overparametrized Models. In *Proceedings of Thirty Third Conference on Learning Theory*, pp. 3635–3673. PMLR, July 2020. URL <https://proceedings.mlr.press/v125/woodworth20a.html>. ISSN: 2640-3498.
- Wu, S., Zhang, H. R., and Ré, C. Understanding and Improving Information Transfer in Multi-Task Learning, May 2020. URL <http://arxiv.org/abs/2005.00944>. arXiv:2005.00944 [cs].
- Yuan, M. and Lin, Y. Model selection and estimation in regression with grouped variables. *Journal of the Royal Statistical Society: Series B (Statistical Methodology)*, 68(1):49–67, 2006. ISSN 1467-9868. doi: 10.1111/j.1467-9868.2005.00532.x. URL <https://onlinelibrary.wiley.com/doi/abs/10.1111/j.1467-9868.2005.00532.x>. eprint: <https://onlinelibrary.wiley.com/doi/pdf/10.1111/j.1467-9868.2005.00532.x>.
- Zhang, Y. and Yang, Q. A Survey on Multi-Task Learning. *IEEE Transactions on Knowledge and Data Engineering*, 34(12):5586–5609, December 2022. ISSN 1558-2191. doi: 10.1109/TKDE.2021.3070203. Conference Name: IEEE Transactions on Knowledge and Data Engineering.
- Zhou, C., Li, Q., Li, C., Yu, J., Liu, Y., Wang, G., Zhang, K., Ji, C., Yan, Q., He, L., Peng, H., Li, J., Wu, J., Liu, Z., Xie, P., Xiong, C., Pei, J., Yu, P. S., and Sun, L. A Comprehensive Survey on Pretrained Foundation Models: A History from BERT to ChatGPT, May 2023. URL <http://arxiv.org/abs/2302.09419>. arXiv:2302.09419 [cs].

A Derivation of the norm minimization bias of PT+FT for diagonal linear networks

We provide a derivation of the norm minimization biases of diagonal linear networks; note that the same result is proved in [Azulay et al. \(2021\)](#).

Recall the parameterization of single-output diagonal linear networks $f : \mathbb{R}^d \rightarrow \mathbb{R}$:

$$f_w(\vec{x}) = \vec{\beta}(\vec{w}) \cdot \vec{x}, \quad \vec{\beta}(\vec{w}) \in \mathbb{R}^D, \quad (6)$$

$$\beta_d(\vec{w}) := w_{+,d}^{(2)} \circ w_{+,d}^{(1)} - w_{-,d}^{(2)} \circ w_{-,d}^{(1)}, \quad (7)$$

where \circ indicates elementwise multiplication.

We proceed by calculating the gradient flow dynamics of the task loss L with respect to the weights \vec{w} . We adopt the notation and strategy of [Woodworth et al. \(2020\)](#). Using the notation $\tilde{X} = [X \ -X]$, we have:

$$\begin{aligned} \dot{\vec{w}}^{(1)}(t) &= \nabla_{\vec{w}^{(1)}(t)} L \\ &= \nabla_{\vec{w}^{(1)}(t)} \left(\|\tilde{X} \left(\vec{w}^{(1)}(t) \circ \vec{w}^{(2)}(t) \right) - y\|_2^2 \right) \\ &= -2\tilde{X}^\top r(t) \circ \vec{w}^{(2)}(t) \end{aligned} \quad (8)$$

$$\begin{aligned} \dot{\vec{w}}^{(2)}(t) &= \nabla_{\vec{w}^{(2)}(t)} L = \nabla_{\vec{w}^{(2)}(t)} \left(\|\tilde{X} \left(\vec{w}^{(1)}(t) \circ \vec{w}^{(2)}(t) \right) - y\|_2^2 \right) \\ &= -2\tilde{X}^\top r(t) \circ \vec{w}^{(1)}(t) \end{aligned} \quad (9)$$

If we change coordinates and define $\vec{s} = \frac{1}{2} (\vec{w}^{(1)} + \vec{w}^{(2)})$ and $\vec{d} = \frac{1}{2} (\vec{w}^{(1)} - \vec{w}^{(2)})$ we have:

$$\dot{\vec{s}}(t) = -2\tilde{X}^\top r(t) \circ \vec{s}(t), \quad (10)$$

$$\dot{\vec{d}}(t) = 2\tilde{X}^\top r(t) \circ \vec{d}(t). \quad (11)$$

$$(12)$$

The solutions to these equations are

$$\vec{s}(t) = \vec{s}(0) \circ \exp \left(-2\tilde{X}^\top \int_0^t r(s) ds \right) \quad (13)$$

$$\vec{d}(t) = \vec{d}(0) \circ \exp \left(2\tilde{X}^\top \int_0^t r(s) ds \right) \quad (14)$$

We are interested in the form of the solution $\vec{\beta}$:

$$\vec{\beta}_{\vec{w}}(t) = w_+^{(1)}(t)w_+^{(2)}(t) - w_-^{(1)}(t)w_-^{(2)}(t), \quad (15)$$

$$= \left((s_+^\rightarrow(t))^2 - (d_+^\rightarrow(t))^2 \right) - \left((s_-^\rightarrow(t))^2 - (d_-^\rightarrow(t))^2 \right), \quad (16)$$

$$= \left((s_+^\leftarrow(t))^2 - (s_-^\leftarrow(t))^2 \right) - \left((d_+^\leftarrow(t))^2 - (d_-^\leftarrow(t))^2 \right). \quad (17)$$

We now make the assumption that the weights are initialized with $\vec{w}_+(0) = \vec{w}_-(0) = \vec{w}_0$ and define $\vec{s}_0 = \frac{1}{2} \left(w_0^{(1)} + w_0^{(2)} \right)$ and $\vec{d}_0 = \frac{1}{2} \left(w_0^{(1)} - w_0^{(2)} \right)$. Then,

$$\begin{aligned}
 \vec{\beta}_{\vec{w}}(t) &= 2\vec{s}_0^2 \circ \exp\left(-4X^\top \int_0^t r(s)ds\right) \\
 &\quad - 2\vec{s}_0^2 \circ \exp\left(4X^\top \int_0^t r(s)ds\right) \\
 &\quad - 2\vec{d}_0^2 \circ \exp\left(4X^\top \int_0^t r(s)ds\right) \\
 &\quad + 2\vec{d}_0^2 \circ \exp\left(-4X^\top \int_0^t r(s)ds\right)
 \end{aligned} \tag{18}$$

$$= 2(\vec{s}_0^2 + \vec{d}_0^2) \cdot \sinh\left(-4X^\top \int_0^t r(s)ds\right) \tag{19}$$

$$= \left(((w_0^{(1)})^2 + ((w_0^{(2)})^2) \right) \cdot \sinh\left(-4X^\top \int_0^t r(s)ds\right) \tag{20}$$

Now the solution is in the same form equation (17) of in Appendix D of [Woodworth et al. \(2020\)](#), but with the coefficient in front of the sinh term replaced by $\left(((w_0^{(1)})^2 + ((w_0^{(2)})^2) \right)$. Following the rest of their argument, it follows that under the assumption that $\vec{\beta}(\infty)$ fits the training data with zero error, among all such solutions, $\vec{\beta}(\infty)$ minimizes the penalty

$$\begin{aligned}
 \|\beta_d\|_Q &:= \sum_{d=1}^D \left(((w_0)_d^{(1)})^2 + ((w_0)_d^{(2)})^2 \right) \\
 &\quad \times q\left(\frac{2\beta_d}{((w_0)_d^{(1)})^2 + ((w_0)_d^{(2)})^2}\right), \\
 q(z) &= 2 - \sqrt{4 + z^2} + z \cdot \operatorname{arcsinh}(z/2)
 \end{aligned} \tag{21}$$

If we assume that the initialization of $w_0^{(2)}$ is a vector with constant entries γ and that $w_0^{(1)}$ is obtained from fitting solution to a pretraining task with effective weights $\vec{\beta}^{aux}$, the assumption of constant magnitude α in the initialization of the first and second-layer weights implies $(w_0)_d^{(1)} = \sqrt{|\beta_d^{aux}|}$, the result in Equation 3 follows.

B Derivation of the $\ell_{1,2}$ penalty minimization bias of MTL

B.1 Multi-task diagonal linear networks

Diagonal linear networks with O outputs are parameterized as:

$$f_w(x) = \vec{\beta}(\vec{w})x, \quad \vec{\beta}(\vec{w}) \in \mathbb{R}^{O \times D}, \tag{22}$$

$$\beta_{o,d}(\vec{w}) := w_{+,o,d}^{(2)} \circ w_{+,d}^{(1)} - w_{-,o,d}^{(2)} \circ w_{-,d}^{(1)}. \tag{23}$$

where \circ indicates elementwise product. We are interested in how minimizing the total parameter norm

$$\begin{aligned}
 &\sum_{d=1}^D \left((w_{+,d}^{(1)})^2 + \sum_{o=1}^O (w_{+,o,d}^{(2)})^2 \right) \\
 &\quad + \left((w_{-,d}^{(1)})^2 + \sum_{o=1}^O (w_{-,o,d}^{(2)})^2 \right)
 \end{aligned} \tag{24}$$

maps to minimizing a norm over the solution weights $\vec{\beta}$. First we note that in the minimum parameter norm solution, for a given input dimension d , either all its associated + weights or all its associated - weights will be zero. Without loss of generality we may assume that all the - weights are zero. So we are to minimize

$$\sum_{d=1}^D \left((w_{+,d}^{(1)})^2 + \sum_{o=1}^O (w_{+,o,d}^{(2)})^2 \right) \quad (25)$$

For given solution coefficients $\vec{\beta}_d \in \mathbb{R}^O$, the value of the input weight $(w_{+,d}^{(1)})^2$ is a free parameter $z_d^2 > 0$, as we can set $w_{+,o,d}^{(2)} := \beta_{o,d}/z$. As any value for z_d leads to the same function, we choose z_d to minimize

$$((w_{+,d}^{(1)})^2 + \sum_{o=1}^O (w_{+,o,d}^{(2)})^2 = z_d^2 + \|\vec{\beta}_d\|_2^2/z_d^2. \quad (26)$$

Setting the derivative to zero implies

$$z_d^2 = \|\vec{\beta}_d\|_2. \quad (27)$$

As a result,

$$\sum_{d=1}^D \left((w_{+,d}^{(1)})^2 + \sum_{o=1}^O (w_{+,o,d}^{(2)})^2 \right) = 2 \sum_{d=1}^D \|\vec{\beta}_d\|_2, \quad (28)$$

where the right-hand side of the equation is the $\ell_{1,2}$ norm.

Note that this implies, as a special case, that the minimum parameter solution to a diagonal linear network with one output minimizes the ℓ_1 norm.

B.2 Multi-task ReLU networks

Multi-task ReLU networks with a shared feature layer and O outputs can be written as

$$f_w(x) = \sum_{h=1}^H w_h^{(2)} (\langle w_h^{(1)}, \vec{x} \rangle)_+ = \sum_{h=1}^H \vec{m}_h (\langle \vec{\theta}_h, \vec{x} \rangle)_+, \quad (29)$$

$$\vec{m}_h = w_h^{(2)} \|w_h^{(1)}\|_2, \vec{\theta}_h = w_h^{(1)} / \|w_h^{(1)}\|_2, \quad (30)$$

where $w_h^{(2)}, \vec{m}_h \in \mathbb{R}^O$. As above, we are interested in how minimizing the parameter norm $\sum_{h=1}^H \|w_h^{(1)}\|_2^2 + \|w_h^{(2)}\|_2^2$ maps to minimizing a norm over the solution weights \vec{m} . For a given $\vec{m}_h \in \mathbb{R}^O$, the norm of the input weight $\|w_h^{(1)}\|_2$ is a free parameter $z_h > 0$, as we can set $w_h^{(2)} := m_h/z$. As any value for z_h leads to the same function, we choose z_h so as to minimize

$$\|w_h^{(1)}\|_2^2 + \|w_h^{(2)}\|_2^2 = z_h^2 + \|\vec{m}_h\|_2^2/z_h^2, \quad (31)$$

Setting the derivative to zero implies

$$z_h^2 = \|\vec{m}_h\|_2. \quad (32)$$

As a result,

$$\sum_{h=1}^H \|w_h^{(1)}\|_2^2 + \|w_h^{(2)}\|_2^2 = 2 \sum_{h=1}^H \|\vec{m}_h\|_2, \quad (33)$$

where the right-hand side of the equation is the $\ell_{1,2}$ norm.

C Comments on cross-entropy vs. mean squared error loss

Cross-entropy and mean squared error are among the most common loss functions in machine learning. An important difference between them is that while mean squared error can be minimized to zero exactly by interpolating the data, cross-entropy achieves its minimum asymptotically as the model predictions become infinitely large (Gunasekar et al., 2018). Consequently, while mean squared error is more amenable to an analysis of the full learning trajectory (Braun et al., 2022), cross-entropy is often more easily understood in the asymptotic limit of infinite training. For homogeneous networks, it has been shown that crossentropy induces an implicit regularization towards the minimal parameter ℓ_2 -norm (Lyu & Li, 2020; Nacson et al., 2019). Because all the networks we consider are homogeneous, by the results of Appendix B, diagonal neural networks trained on multiple tasks with crossentropy loss for infinite time would indeed minimize the $\ell_{1,2}$ -norm, and ReLU networks would minimize the $\mathcal{F}_{1,2}$ -norm. However, PT+FT

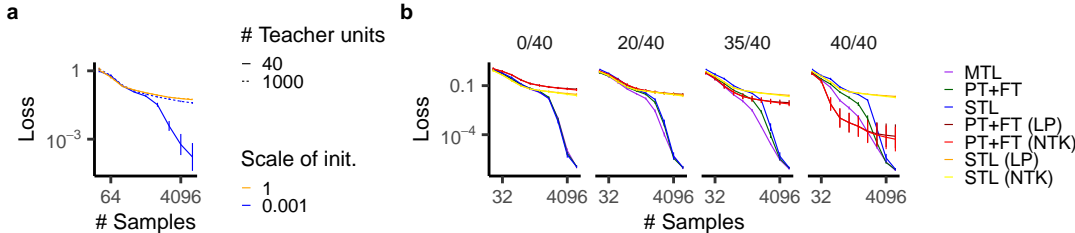


Figure 4: Larger-scale teacher-student experiments. **a**, Generalization loss of shallow ReLU networks trained on data from a ReLU teacher network (as in Fig. 2, except with more teacher units and more data). **b**, Generalization loss for different numbers of overlapping features (out of 40 total) between main and auxiliary tasks. NTK indicates the (lazy) tangent kernel solution. This is comparable to Fig. 2a, except with more teacher units and more data.

networks would minimize the ℓ_1 and \mathcal{F}_1 norms, respectively, behaving identically to single-task learning. This is because given infinite training time, the behavior of networks trained with cross-entropy loss is in theory independent of initialization. This behavior is quite different from that of networks trained with mean squared error loss at convergence, which is heavily dependent on initialization (indeed, this is the basis of our investigation in this work). However, prior work has shown that given finite training time, networks trained on cross-entropy loss learn solutions that are sensitive to initialization, and indeed there is a correspondence between increasing training time and decreasing initialization scale (incentivizing rich / feature-learning behavior). Thus, we expect our qualitative findings are applicable to the case of networks trained with cross-entropy loss for finite time. Moreover, our results on the effects of rescaling network parameters (e.g. to uncover the nested feature-selection regime) may be able to be replicated in the cross-entropy setting by scaling training time.

D Robustness of main results to choice of number of auxiliary task samples and input dimension

To increase confidence that our main results are robust to the number of data samples used (1024 auxiliary task samples and up to 1024 main task samples in most of our experiments), and the number of ground-truth units in the teacher network (6), we repeated the experiments of Fig. 2a with 8192 auxiliary task samples and 40 ground-truth features. Indeed, in this setting the rich regime also helps with generalization if and only if the teacher units are sparse (Fig. 4a). Further, MTL and PT+FT tend to outperform STL if the features are overlapping and MTL tends to outperform PT+FT (Fig. 4b). In particular, the finetuned networks still benefit from feature learning, especially if some features are novel.

E Analysis of learned solutions in linear and nonlinear networks

Our linear theory predicts inductive biases towards solutions that minimize norms, often either ℓ_1 -like (incentivizing sparsity) or ℓ_2 -like. Our experiments in Fig. 2 corroborate these description by analyzing how sample complexity depends on the feature sparsity of the ground-truth task solution, and how the sparse feature structures of the main and auxiliary tasks relate. However, this evidence for sparsity biases (or lack thereof) is indirect; here we present more direct analyses of the learned solutions in linear and nonlinear networks that support the account we provide in the main text.

E.1 Diagonal linear networks

To check whether the implicit regularization theory is a good explanation for these performance results, we directly measured the $\ell_{1,2}$ and Q norms of the solutions learned by networks, compared to the corresponding penalties of the ground truth weights. In Fig. 5a we see that as the amount of training data increases, the norms all converge to that of the ground truth solution, but in the low-sample regime, MTL and PT+FT find solutions with lower values of their corresponding norm than the ground-truth function, consistent with the implicit regularization picture (by contrast, STL does not consistently find solutions with lower values of these norms than the ground truth).

Our theory predicts that weight rescaling by a factor less than 1.0 following pretraining reduces the propensity of the network to share features between auxiliary and main tasks during finetuning. We confirm that this is the case in Fig. 5b by analyzing the overlap between the auxiliary task features and the learned linear predictor for the main task.

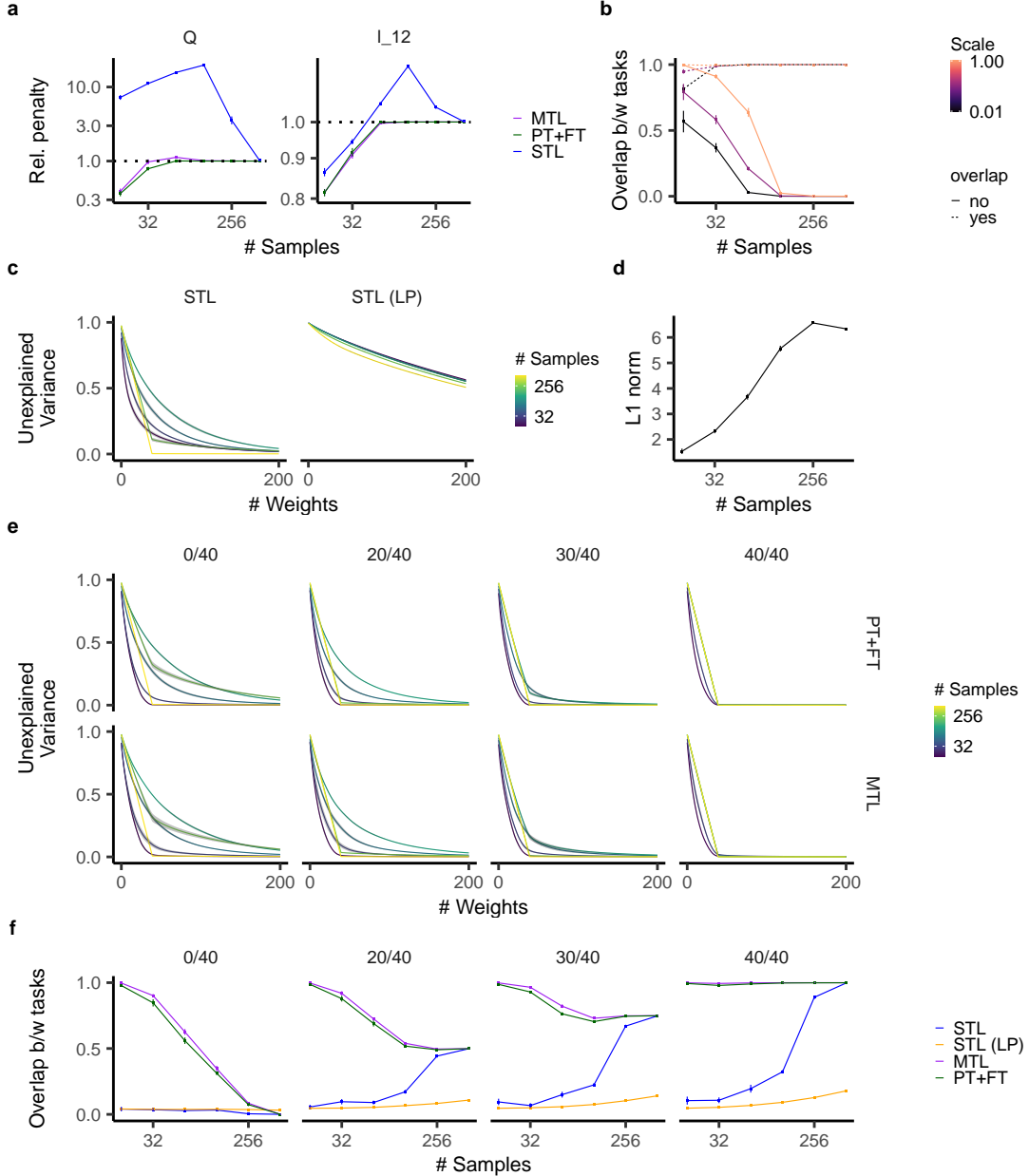


Figure 5: **a**, $\ell_{1,2}$ norm and Q penalty for MTL, STL, and PT+FT networks from Fig. 1a (40/40 overlapping features case). **b**, Proportion of the weight norm in the 40 dimensions relevant for the auxiliary task, for the networks in Fig. 1i. Weight rescaling decreases this overlap. **c**, Proportion of variance concentrated in the top k weights, as a function of k , for training on a single-task. When both layers are trained from small initialization (STL), this variance decreases much more rapidly than for pure linear readout training (STL (LP)), demonstrating the sparsity of the learned solution. **d**, L1 norm for STL as a function of the number of samples. **e**, Proportion of variance across different overlaps and for different learning setups (see also Fig. 1c). The rapid decrease in variance demonstrates the sparsity of the learned solutions both for PT+FT and MTL. **f**, Proportion of weight norm in the 40 dimensions relevant for the auxiliary task (see also Fig. 1d).

In Fig. 5c we show that our measure of effective sparsity of learned solutions in diagonal linear networks effectively distinguishes between networks trained in the feature selection regime and networks trained with linear probing (only training second-layer weights). Moreover, in Fig. 5d we show that the L1 norm of the solution increases with the training sample size, consistent with a bias towards L1 minimization. There is an interesting discrepancy between the behavior of the sparsity of the solutions (nonmonotonic, see Fig. 5c) and the L1 norm (largely monotonic, see Fig. 5d).

This is attributable to the discrepancy between the L1 norm (which diagonal linear networks in the rich regime are biased to minimize) and sparsity (for which L1 norm is only a proxy).

In Fig. 5e we show the same information as Fig. 1c but for different values of the number of overlapping features between main and auxiliary tasks (each of which uses 40 features). We find that, as in the example shown in the main text, learned solutions across a range of overlaps are as sparse as using single-task learning (see fig. 5c) when task features do not overlap (0/40 case) and more sparse otherwise (on account of the bias toward reuse of the sparse features learned during the auxiliary task, see next paragraph).

In Fig. 5f we show the same information as Fig. 1d but for different values of the number of overlapping features between main and auxiliary tasks (each of which uses 40 features). We find that, as in the example shown in the main text, learned main task solutions are biased to share auxiliary task features when few samples are available.

E.2 ReLU networks

We adopt a clustering-based approach to analyzing the effective sparse structure of learned task solutions. Specifically, for a given trained network, we perform k-means clustering with a predetermined value of K clusters on the normalized input weights to each hidden-layer neuron in the network³. We measure the extent to which K cluster centers are able to explain the variance in input weights across hidden units; the fraction of variance left unexplained is commonly referred to as the “inertia.” For values of K at which the inertia is close to zero, we can say that (to a good approximation) the network effectively makes use of at most K nonlinear features.

E.2.1 Single-task learning: rich inductive bias yields clusters of similarly tuned neurons that approximate sparse ground-truth features

In the single-task learning case, we measure the inertia of trained networks in Fig. 2d as a function of K . We find that for networks in the rich regime (small initialization scale), for tasks with sparse ground-truth (six units in the ReLU teacher network), the networks do indeed learn solutions that make use of approximately six nonlinear features (Fig. 6a). For tasks with many (1000) units in the teacher network, the network finds solutions that use a small number of feature clusters when main task samples are limited, but gradually uses more clusters as the number of samples is increased (Fig. 6a), at which point the network matches the teacher function very well, see Fig. 2d). This bias towards sparser-than-ground-truth solutions given insufficient data corroborates our claim of an inductive bias towards sparse solutions. By contrast, networks in the lazy learning regime (large initialization scale) display no such bias, corroborating our claim that the sparse ℓ_1 -like inductive bias is a property of the rich regime but not the lazy regime. Interestingly, in the sparse ground-truth case learned solutions are relatively less sparse for an intermediate number of training examples. This may arise because an ℓ_1 -like inductive bias is not exactly the same as a bias toward sparse solutions over nonlinear features, particularly when training data is limited. We leave an in-depth investigation of this phenomenon to future work.

Our clustering analysis allows us to measure the extent to which the effective features employed by the network (cluster centers) are aligned with the ground-truth task features. Specifically, for each teacher unit, we compute an “alignment score” between teacher and student networks by taking each teacher unit, measuring its cosine similarity with all the cluster centers, choosing the maximum value, and averaging this quantity across all teacher units. We find that the learned feature clusters are indeed highly aligned with the ground-truth teacher features in the sparse ground-truth case, and moreso as the number of main task samples (and consequently task performance) increases (Fig. 6b).

E.2.2 Pretraining+finetuning finds sparse solutions and improves alignment of feature clusters learned during pretraining

We find that pretraining+finetuning improves performance over single-task learning when main and auxiliary task features are shared (or correlated), and maintains an apparent bias toward sparsity in new task-specific features. To corroborate these claims, we performed our clustering analysis on the solutions learned through PT+FT. We find that the solutions learned are indeed quite sparse (comparable to the sparsity of solutions learned by single-task learning), even when the auxiliary task and main task features are disjoint (Fig. 6c). Moreover, we find that MTL also learns sparse solutions (Fig. 6d). In particular, as expected, the effective features on tasks with overlapping features is equal to the number of total unique features. Moreover, we observe that when main task and auxiliary task features are shared, PT+FT and MTL networks exhibit higher alignment between learned features and ground-truth features than single-task-trained networks, especially when main task samples are limited (Fig. 6e). This provides a mechanistic

³weighting the importance of each unit to the k-means objective by the weight of its contribution to the network’s input-output function, specifically the magnitude of the product of its associated input and output weights

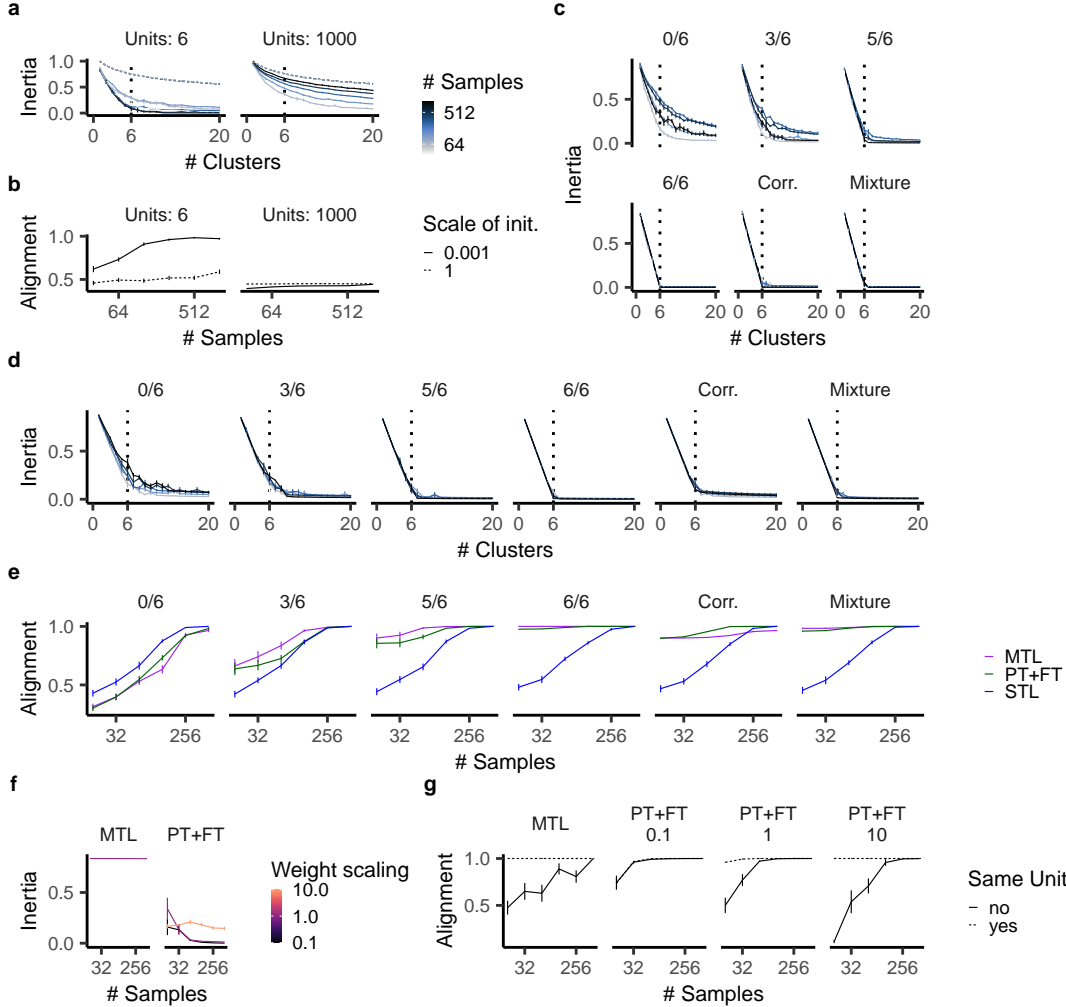


Figure 6: Analysis of effective sparsity of learned ReLU network solutions. **a** Inertia (k-means reconstruction error for clustering of hidden-unit input weights) as a function of the number of clusters used for k -means, for different numbers of main task samples and ground-truth teacher network units, in single-task learning. **b** Alignment score – average alignment (across teacher units) of the best-aligned student network cluster uncovered via k -means. **c**, Inertia for networks trained using PT+FT for the tasks of Fig. 2a and Fig. 2c. **d**, Same as panel c but for networks trained with MTL. **e**, Alignment score for networks trained with MTL, PT+FT, and STL on the same tasks as in panels c and d. **f** Inertia (using $k = 1$ clusters) for networks trained on an auxiliary task that relies on only one ground-truth feature, which is one of the six ground-truth features used in the auxiliary task (as in Fig. 2e,f), using MTL or PT+FT with various rescaling factors applied to the weights prior to finetuning. **g** Alignment score for the networks and task in panel f.

underpinning for the relationship between the inductive bias of PT+FT that we describe in the main text and its performance benefits.

E.2.3 Nested feature selection regime allows network to prioritize a sparse subset of feature clusters learned during pretraining

In the main text we describe the “nested feature selection” regime, which occurs at intermediate values of the ratio between ground-truth main task feature coefficients and pretrained network weight scale. In this regime, networks can more efficiently learn main tasks that make use of a subset of the features used in the auxiliary task (Fig. 1f, Fig. 2e) while still maintaining a bias towards reusing features from the auxiliary task (Fig. 1g, Fig. 2f). Here we show that networks in this regime (obtained most clearly in the shallow ReLU network case when networks are rescaled by a value of 1.0 after pretraining, see Fig. 2e,f) indeed learn very sparse (effectively 1-feature) solutions when the ground-

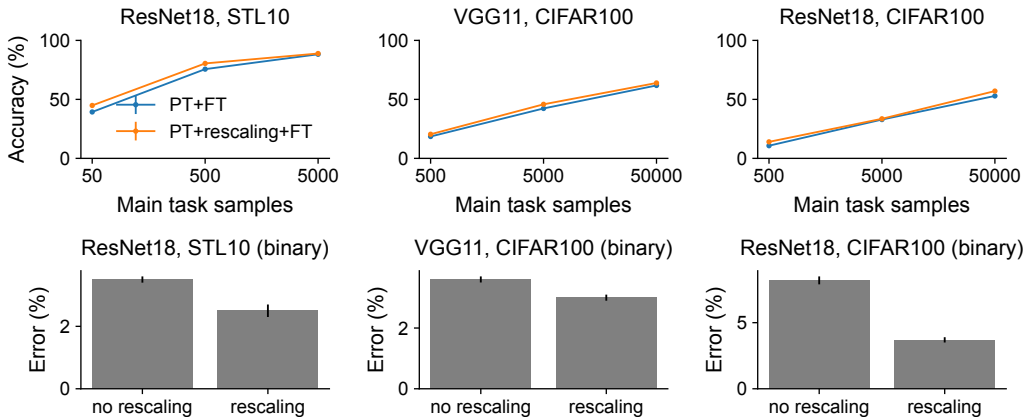


Figure 7: Results for finetuning deep convolutional networks trained on ImageNet, with/without weight rescaling (factor of 0.5) prior to finetuning.

truth main task consists of a single auxiliary task features (Fig. 6e, right). By contrast, networks with weights rescaled by a factor of 10.0 following pretraining exhibit no such nested sparsity bias (consistent with lazy-regime behavior). Similarly, multi-task networks cannot exhibit such a bias in their internal representation as they still need to maintain the features needed for the main task (Fig. 6e, left). Additionally, supporting the idea that the nested feature selection regime allows networks to benefit from feature reuse (Fig. 1i, Fig. 2i), we find that networks in this regime exhibit a higher alignment score with the ground-truth teacher network when the main task features are a subset of the auxiliary task features compared to when they are disjoint from the auxiliary task features (Fig. 6g). This alignment benefit is mostly lost when networks are rescaled by a factor of 0.1 following pretraining (a signature of rich-regime-like behavior).

F Further evaluations of the rescaling method for finetuning

To evaluate the robustness / general-purpose utility of our suggested approach of rescaling network weights following pretraining, we experimented with finetuning convolutional networks pretrained on ImageNet on downstream classification tasks: pretrained ResNet-18 finetuned on CIFAR100, pretrained VGG11 finetuned on CIFAR100, and pretrained ResNet-18 finetuned on STL-10. We experimented both with finetuning on the full multi-way classification task, and also on binary classification tasks obtained by subsampling pairs of classes from the main task dataset (which we found exposes performance differences more strongly). Due to computational constraints, we did not sweep over the choice of the rescaling factor, but simply used a factor of 0.5 in all cases. We find that rescaling improves finetuning performance, to varying degrees, in all of our experiments (Fig. 7).

G Analysis of representations learned in the nested feature selection regime: bridging the gap from shallow to deep networks

We were interested in testing whether our theoretical understanding of shallow networks is truly responsible for the behavior of deeper networks (with more direct evidence than performance results / sample complexity). Specifically, we sought to understand whether the observed benefit of rescaling network weights following pretraining (Fig. 2h, Appendix. F) relates to the nested feature selection regime we characterized in shallow networks. Doing so is challenging, as the space of “features” learnable by a deep network is difficult to characterize explicitly (making the feature clustering analysis employed in Appendix. E inapplicable). To circumvent this issue, we propose a signature of nested feature selection that can be characterized without knowledge of the underlying feature space. Specifically, we propose to measure (1) the *dimensionality* of the network representation pre- and post-finetuning, and (2) the extent to which the representational structure post-finetuning is shared with / inherited from that of the network following pretraining prior to finetuning.

We employ the commonly used *participation ratio* (PR; Gao et al., 2017) as a measure of dimensionality. For an $n \times p$ matrix \mathbf{X} representing n mean-centered samples of p -dimensional network responses, with a $p \times p$ covariance matrix $\mathbf{C}_X = \frac{1}{n} \mathbf{X}^\top \mathbf{X}$, the participation ratio is defined as

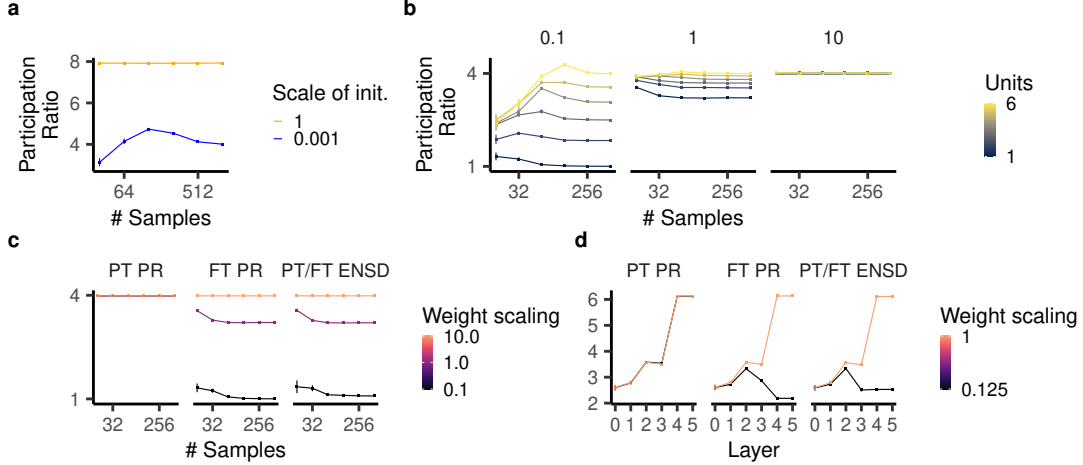


Figure 8: Dimensionality of the network representations before and after finetuning. **a**, Participation ratio of the ReLU networks’ internal representation after training on a task with six teacher units. **b**, Participation ratio of the network representation after finetuning on the nested sparsity task with different weight rescalings. **c**, Participation ratio before (left panel) and after finetuning (middle panel) and the effective number of shared dimensions between the two representations (right panel). Small weight scaling decreases the participation ratio after training. **d**, The same quantities for ResNet18 before and after finetuning (see also Fig. 2h).

$$\begin{aligned}
 PR(X) &= \frac{(\sum_{i=1}^p \lambda_i)^2}{\sum_{i=1}^p \lambda_i^2} = \frac{\text{trace}(\mathbf{C}_X)^2}{\text{trace}(\mathbf{C}_X^2)} \\
 &= \frac{\text{trace}(\mathbf{X}^\top \mathbf{X})^2}{\text{trace}(\mathbf{X}^\top \mathbf{X} \mathbf{X}^\top \mathbf{X})}
 \end{aligned} \tag{34}$$

where λ_i are the eigenvalues of the covariance matrix \mathbf{C}_X . The PR scales from 1 to p and measures the extent to which the covariance structure of responses \mathbf{X} is dominated by a few principal components or is spread across many. We argue that low-dimensional representations are a signature of networks that use a sparse set of features. We confirm that this is the case in our teacher-student setting: networks in the rich regime, which are biased towards sparse solutions, learn representations with lower PR than networks in the lazy regime, which are not biased toward sparse solutions (Fig. 8a).

Our measure of shared dimensionality between two representations is the *effective number of shared dimensions* (ENSD) introduced by Giaffar et al. (2023). The ENSD for an $n \times p$ matrix of responses \mathbf{X} from one network and an $n \times p$ matrix of responses \mathbf{Y} from another network, denoted $ENSD(X, Y)$, is given by

$$\frac{\text{trace}(\mathbf{Y}^\top \mathbf{X} \mathbf{X}^\top \mathbf{Y}) \cdot \text{trace}(\mathbf{X}^\top \mathbf{X}) \cdot \text{trace}(\mathbf{Y}^\top \mathbf{Y})}{\text{trace}(\mathbf{X}^\top \mathbf{X} \mathbf{X}^\top \mathbf{X}) \cdot \text{trace}(\mathbf{Y}^\top \mathbf{Y} \mathbf{Y}^\top \mathbf{Y})} \tag{35}$$

This measure is equal to the centered kernel alignment (CKA), a measure of similarity of two network representations (Kornblith et al., 2019a), multiplied by the geometric mean of the participation ratios of the two representations. It measures an intuitive notion of “shared dimensions” — for example, if \mathbf{X} consists of 10 uncorrelated units, if \mathbf{Y} is taken from a subset of five of those units, the $ENSD(X, Y)$ will be 5. If \mathbf{Y} is taken to be five uncorrelated units that are themselves uncorrelated with all those in \mathbf{X} , the $ENSD(X, Y)$ will be zero.

Intuitively, the PR and ENSD of network representations pre- and post-finetuning capture the key phenomena of the nested feature selection regime. In a case in which the main task uses a subset of the features of the auxiliary task, if the network truly extracts this sparse subset of features, we expect the dimensionality of network after finetuning to be lower than after pretraining ($PR(\mathbf{X}_{FT}) < PR(\mathbf{X}_{PT})$), and for nearly all of the representational dimensions expressed by the network post-finetuning to be inherited from the network state after pretraining ($ENSD(\mathbf{X}_{PT}, \mathbf{X}_{FT}) \approx PR(\mathbf{X}_{FT})$). By contrast, networks not in the nested feature selection regime should exhibit

an ℓ_2 -like rather than ℓ_1 -like bias with respect to features inherited from pretraining and thus not exhibit a substantial decrease in dimensionality during finetuning.

We show that this description holds in our nonlinear teacher-student experiments. Networks that we identified as being in the “nested feature selection” regime (weights rescaled by 1.0 following pretraining), and also networks in the rich regime, exhibit decreased PR following finetuning (Fig. 8b). By contrast, lazy networks (weights rescaled by 10.0 following pretraining) exhibit no dimensionality decrease during finetuning. Additionally (see Fig. 8c), the ENSD between pretrained (PT) and finetuned (FT) networks is almost identical to the dimensionality of the finetuned representation (PR FT).

Strikingly, we observe very similar behavior in our ResNet-18 model pretrained on 98 CIFAR-100 classes and finetuned on the 2 remaining classes (Fig. 8d), when we apply our method of rescaling weights post-finetuning. Analyzing the PR and ENSD of the outputs of different stages of the network following pretraining and following finetuning, we see that dimensionality decreases with finetuning, and ENSD between the pretrained and finetuned networks is very close to the PR of the finetuned network. Moreover, this phenomenology is only observed when we apply the weight rescaling method; finetuning the raw pretrained network yields no dimensionality decrease. These results suggest that the success of our rescaling method may indeed be attributable to pushing the network into the nested feature selection regime.